

Article

Seismic Microzonation Map for a Fixed-Jacket Platform in the Malay Basin

Mohamad Mazlina ^{1,2}, M. S. Liew ¹, Kamaluddeen Usman Danyaro ^{3,*} , Azlan Adnan ⁴
and Nor Hayati Ab Hamid ⁵

¹ Civil and Environmental Engineering Department, Universiti Teknologi PETRONAS, Seri Iskandar 32610, Perak, Malaysia

² School of Civil Engineering, College of Engineering, Universiti Teknologi MARA Selangor, Shah Alam 40450, Selangor, Malaysia

³ Computer and Information Science Department, Universiti Teknologi PETRONAS, Seri Iskandar 32610, Perak, Malaysia

⁴ Faculty of Civil Engineering, Universiti Teknologi Malaysia, Johor Bahru 81310, Johor, Malaysia

⁵ Institute for Infrastructure Engineering and Sustainable Management (IIESM), Universiti Teknologi MARA, Shah Alam 40450, Selangor, Malaysia

* Correspondence: kamaluddeen.usman@utp.edu.my

Abstract: The existence of soft soil in offshore areas may lead to the amplification of vibration received from offshore facilities, especially from the existing fixed-jacket platforms, which were designed without provision to seismicity, as in Malaysian water. Therefore, this study was designed to develop a seismic microzonation map and a soil amplification factor map according to soil type; we propose horizontal response spectra and site coefficient values (C_a and C_v) for the Malay Basin. A one-dimensional nonlinear analysis of layered soil (NERA) was used in the ground response analysis for six selected seismic events under five return periods of 100, 200, 500, 1000, and 2500 years. Soil amplification factors for soil types D and E showed a decreasing trend from 100 years to 2500 years. Two designed horizontal response spectra are proposed (for soil type D and E) under average and envelope conditions; a comparison with ISO showed that the proposed spectra were higher, especially for soil type E. To summarize, the seismicity effect should be included in the development of offshore industries as findings indicated that soil amplification occurred in soil types D and E at the Malay Basin.

Keywords: seismicity; seismic microzonation; microzonation map; ground response analysis; offshore facilities in the Malay Basin



Citation: Mazlina, M.; Liew, M.S.; Danyaro, K.U.; Adnan, A.; Hamid, N.H.A. Seismic Microzonation Map for a Fixed-Jacket Platform in the Malay Basin. *Appl. Sci.* **2022**, *12*, 9194. <https://doi.org/10.3390/app12189194>

Academic Editor: Fabrizio Balsamo

Received: 25 May 2022

Accepted: 7 September 2022

Published: 14 September 2022

Publisher's Note: MDPI stays neutral with regard to jurisdictional claims in published maps and institutional affiliations.



Copyright: © 2022 by the authors. Licensee MDPI, Basel, Switzerland. This article is an open access article distributed under the terms and conditions of the Creative Commons Attribution (CC BY) license (<https://creativecommons.org/licenses/by/4.0/>).

1. Introduction

The seismicity of the continental shelf of Malaysia is believed to be affected by its surrounding active faults and subduction zone. Malaysia is located on the Eurasian Plate and in the vicinity of two seismically-active plate boundaries. These boundaries are the inter-plate boundary between Eurasian and Philippine Plates on the east side while the inter-plate boundary is between the Indian–Australian and Eurasian Plates on the west side of Malaysia. Previous study highlighted that the Indian Ocean plate is moving at an estimated velocity of 7 cm/year toward the northeast and subducts under the Sumatra in the west of Malaysia [1]. Furthermore, the Philippine Plate is moving at an estimated 8 cm/year toward Malaysia, which might cause several micro-faults in Sabah. It was reported that Malaysia might be (and has been) affected by large tremor events in and around these boundaries [1].

In 2005, the nearest distance of the earthquake epicenter from Malaysia was approximately 350 km; this earthquake type could normally cause significant damage within a 100–200 km radius from the epicenter [2]. Even though Malaysia is out of the range,

two large earthquakes near Sumatra, which occurred at the end of 2002 ($M_w = 7.4$) and in early 2003 ($M_w = 5.8$), caused tremors, which were felt by several cities in Peninsular Malaysia, including Penang and Kuala Lumpur. Few building cracks have been reported in Penang due to the 2002 Northern Sumatra earthquake [3]. After the fatal incident of the Sumatra Earthquake ($M 9.2$) in 2004, the global seismicity patterns have been affected by other earthquake events that struck the East Indian Ocean on 11 April 2012, at $M 8.6$. These earthquake events caused long-distance earthquake tremors or far-field effects, which could be felt, leading to panic in several cities in Peninsular Malaysia. Details of the seismicity around Java, Indonesia, was discussed in detail in previous research [4].

Despite its distance of the earthquake epicenter, Malaysia has a local epicenter (mainly in Sabah). Several possible active faults have been outlined and local earthquakes in East Malaysia seem to be related to some of them (seismic events from surroundings). Several possible active faults, such as the Mensaban and Loubo-Loubo, have been identified, and local earthquakes in East Malaysia seem to be related to some of these fault lines. From the observation based on the Modified Mercalli (MM) intensity scale, the maximum intensities for West and East Malaysia are VI and VII, respectively [1]. MM VI represents strong shaking, where shaking can be felt and cause slight damage, while VII represents very strong shaking, were negligible, and slight to moderate damage; damage can be seen in the structure depending on its design.

PETRONAS Carigali Sdn. Bhd. (PCSB) has been entrusted to manage the hydrocarbon resources available in Malaysia. Operation areas offshore were divided into three, which are known as Peninsular Malaysia operation (PMO), Sabah operation (SBO), and Sarawak operation (SKO). There are many platforms available for offshore operation, such as a fixed-jacket platform, compliant tower, SPAR platform, and tension leg platform. However, all fixed-jacket platforms are widely used all over the world. This type of platform is meant for shallow water depths where the maximum depth is around 400 to 500 m [5]. The foundation of this platform has direct contact with the seabed. Thus, there is a need to determine the seismic microzonation map for the Malay Basin that can be used in the development and maintenance of offshore facilities.

The Malay Basin as shown in Figure 1 is located in the South China Sea and consists of more than 150 hydrocarbon resource discoveries in 2003. The oil exploration started in the late 1960s; thus, numerous offshore facilities are available in the basin. The length and width of Malay Basin are about 500 and 200 km, respectively [6–9]. The location of the Malay Basin is depicted, and the distribution of oil and gas fields is portrayed. The Malay Basin is part of PMO under the PCSB operation. The history of offshore hydrocarbon exploration for the Malay Basin was elaborated by Ramli (1985) [8]. The Malay Basin is considered shallow water; the water depth is less than 200 m.

Seismicity in the Malay Basin was highlighted by previous researchers where the existence of folds and faults in the Malay Basin were highlighted in [6–8,10–12]. The existence of inactive old faults cannot be ignored as they have the potential to be active again due to the pull and push activities of the plates that can build more stresses beneath the surface, which sometimes need to be released. Offshore facilities in the Malay Basin might be in danger if it happens. Furthermore, concerns about the existence of aging platforms in the Malay Basin have also been highlighted by previous researchers [13–15]. The development of the Malay Basin before hydrocarbon resources is an ongoing process where maintenance and new development will be carried out. Thus, the Malay Basin is the area of interest in this study.

Seismicity can normally be assessed by a seismic hazard map (produced based on natural or geotechnical hazards). Natural hazards in seismic hazard maps represent the kind of hazards that affect the site itself, for example, ground motion and liquefaction. Geotechnical hazards represent the influence of natural hazards on engineering objects at certain locations. Some examples of geotechnical hazards involve the effects of liquefaction, slope stability, and ground motion on engineering structures [16]. A seismic hazard map for ground motion can be produced based on a macrozonation or microzonation map. Please

note that macrozonation here is about presenting the dynamic parameters, such as peak ground acceleration and spectral acceleration on the bedrock in the seismic hazard map, while microzonation is the addition of local soil conditions to macrozonation where the influence on the surface can be obtained and presented in the seismic hazard map [16]. In microzonation, the effect of soil layers beneath the surface is also included.

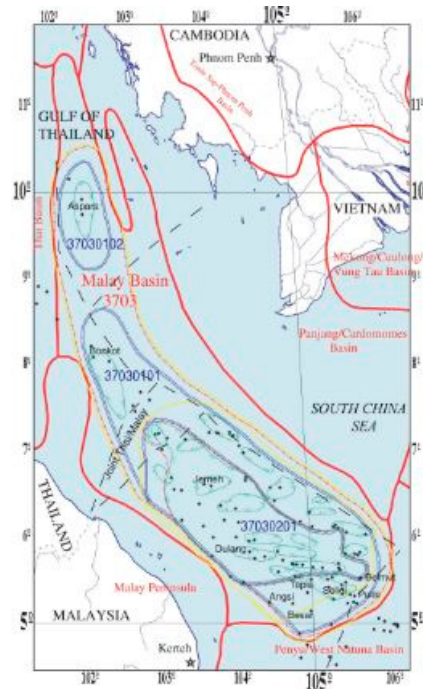


Figure 1. Malay Basin in South China Sea [6].

Govindaraju et al. (2004) [17], dealing with the existence of seismic hazards, highlighted that the estimation of the site-specific dynamic response of a layered soil deposit must be executed. Beyhan et al. (2017) [18] claimed that in any seismic soil structure study, the site response analysis will normally be the first step. The site response analysis or ground response analysis (GRa) helps engineers to calculate the natural period for a site, assess amplification of ground motion, and determine various parameters, such as response spectra, which will be used in designing and evaluating structure safety [17].

Methods to analyze GRa can be broadly grouped into linear analysis, equivalent linear analysis, and nonlinear analysis. Linear analysis is the most common method used for GRa due to its simplicity [17]. In linear analysis, the soil is considered a uniform layer with either constant or varying soil stiffness over depth. Thus, it can be expressed by a simple mathematical function. However, in reality, material properties of soil will change in space, and soil does not have elastic behavior. Hence, finite difference and finite elements, which are in the numerical method, must be used.

Equivalent linear analysis was discussed by Basu and Dey (2016). In equivalent linear analysis, equivalent linear properties, such as shear modulus, are used in the approximation of a non-linear hysteric stress–strain behavior of soil under cyclic loading. Normally, the effective shear strain value for GRa is set at 65% of the peak shear strain of an earthquake motion. The nonlinear analysis involves analyzing soil layers or deposits by implementing numerical integration of the time domain in small steps. Any nonlinear stress–strain model developed according to Masing and non-Masing rules can be incorporated during the integration process. In each time step, soil properties for the next iteration will be assumed or calculated by referring to the stress–strain relationship. Thus, stress–strain characteristics for the soil must be modeled realistically to ensure meaningful results of the analysis [17,19]. The advantages of using the nonlinear analysis method were discussed by previous researchers [20–22].

The GRa method normally utilizes a shear wave propagation approach that comprises of one-dimensional (1D), two-dimensional (2D), and three-dimensional (3D) analysis. In the seismic code for the engineering structure, 1D is widely used compared to the other two methods [17,20]. GRa involving 2D and 3D methods will normally be used under special requests since more input data will be necessary. Further discussions are provided for the 1D method. The nonlinearity of soil material is represented by using either equivalent linear or nonlinear methods. In the 1D method, there are several assumptions made where the length of the soil will be ignored, and the soil boundary is assumed horizontal but the thickness will be accounted [22].

From the literature that was reviewed, parameters of seismic waves, such as duration, amplitude, and frequency can be influenced by the soil condition and local site effect as the wave propagates upward through the soil layers from the bedrock up to the soil surface [23]. Based on Kramer (1996) [24], the seismic wave can either be amplified or de-amplified depending on the soil deposit parameters, such as soil density, thickness, and type. Adrian et al. (2000) [25] highlighted that the natural period of the site has a significant influence on the amplification of ground motion. High vibration will occur when the seismicity and site share the same frequency.

Soil amplification may occur in the area of soft soil, and it is known that the offshore area normally consists of soft soil. The amplification of each site will depend on the combination of soil and thickness of each layer. The range and value of the soil amplification factor varied at different locations. It shows the importance of obtaining soil amplification factors for specific areas to avoid the under- or over-design of engineering structures. Thus, in the current study, the soil amplification factor was determined for the Malay Basin where a lot of offshore facilities are operating.

Most of the offshore platforms in Malaysian water were designed based on API, ISO, and PTS codes of practice. The conventional method was also adopted by ISO 19901-2 in plotting response spectra, as shown in Figure 2. This method was adopted in the current study, in accordance with ISO 19901-2, except for the spectral accelerations of 0.2 s and 1.0 s. In constructing the response spectrum for Malaysian water using ISO 19901-2, 5% damping was assumed and the values of the spectral accelerations for 0.2 s and 1.0 s periods are provided in Figure 3. Spectral acceleration in ISO 19901-2 for 0.2 s is 0.05 g while 1.0 s is 0.02 g for the 5% damping ratio.

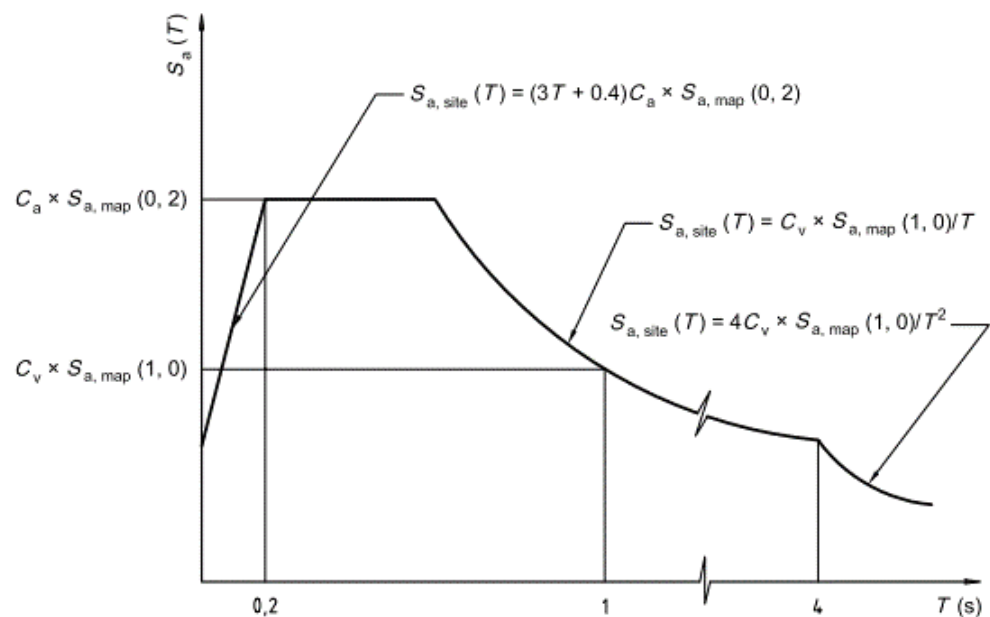


Figure 2. Damping [26].

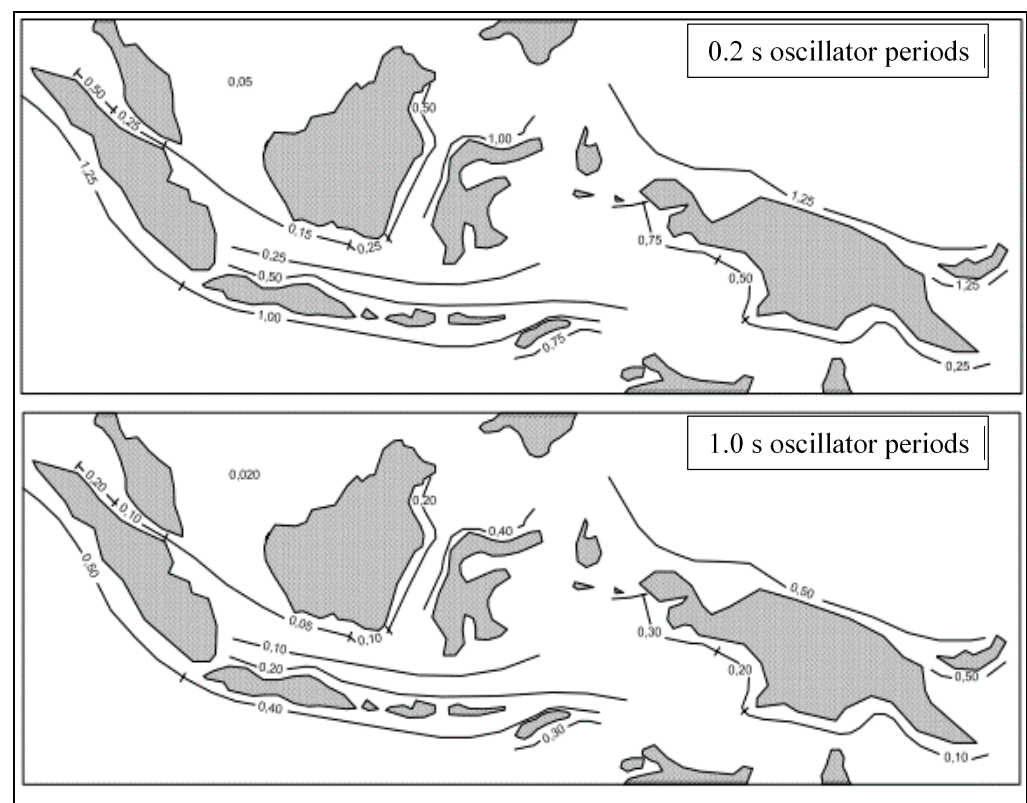


Figure 3. Map of 5% damping spectral response acceleration for offshore Indonesia [26].

According to Freeman (2007) [27], the usefulness of response spectra as a tool in the design and analysis process increased due to the requirement of building codes and acceptable performance-based design (PBD) techniques. Thus, many studies were conducted on previous researchers' spectral responses due to seismic excitation, and the influence on the structure was also highlighted. Freeman (2007) [27] discussed how seismic design forces can be obtained from design response spectra for both low-rise and high-rise buildings. They also highlighted that the estimation of a smooth spectrum is reasonable if the average of the maximum and minimum curves were used.

Chang et al. (2005) [28] studied the comparisons of ISO and API seismic designs for three offshore platforms. Before that, plotting was conducted of seismic acceleration response spectra for the 5% damping ratio based on ISO for different size classes; it can be seen that the types of soil governed the period of a specific site. The highest acceleration started at 0.2 s and the period of constant acceleration increased from harder soil to softer soil; from site class A/B to site class E (Chang et al. 2005 [28]; Villaverde, 2009 [29]). This response spectrum can also be plotted using a log–log scale. In the current study, the conventional method was adopted where design response spectra (with respect to period) were plotted based on ISO.

From the literature reviewed, the existence of an aging platform in the Malay Basin was designed without provision for seismicity, and the seismicity in the Malay Basin and surroundings raised concerns from researchers. Furthermore, an offshore area normally consists of soft soil that has the potential of having a soil amplification effect that will increase the amount of the vibration received by the surface. It is still questionable whether the Malay Basin experiences an amplification effect or not. Thus, the aim of this study was to determine the seismic microzonation map, the map of soil amplification factors, designed horizontal response spectra, and site coefficients of selected sites in the Malay Basin.

2. Materials and Methods

There were three phases of the research methodology for this study to address the three objectives. Phase one addresses the first objective, which is to develop a seismic microzonation map of the Malay Basin for offshore facilities. It consists of a data collection process for ground response analysis input, such as seismic time histories, peak ground acceleration, and soil properties. During this phase, one developed program, known as the nonlinear earthquake site response analysis of layered soil deposits (NERA), has been adopted. This one-dimensional nonlinear analysis produced output, such as peak surface acceleration (PSa) and response spectra (RS). Peak surface accelerations were analyzed to develop seismic microzonation mapping for the Malay Basin to address objective number one.

Phase two of this study addresses the second objective. PSa was used to determine soil amplification factors. The obtained soil amplification factors were used to produce maps of soil amplification factors for the Malay Basin. In phase three, horizontal RS were analyzed to produce design horizontal response spectral acceleration and site coefficient values (C_a and C_v) for soil types D and E of the available data in the Malay Basin to address objective number three. As stated in ISO 19901-2 [26], soil type D represents stiff to very stiff soil, while soil type E is classified as soft to firm soil. Soil classification in this study is based on the average soil shear wave velocity (V_s) of the top 30 m of the seabed. Equation (1) was used in determining V_s for the study area. The detailed flowchart for this research methodology is shown in Figure 4.

$$V_s = 30 / \sum_{i=1}^n \frac{d_i}{V_{s,i}} \quad (1)$$

2.1. Phase One: Development of Seismic Microzonation Map

This phase was designed to collect data for the input in the ground response analysis (GRa). GRa is a process where the reaction of soil layers under vibration, as an example, can be predicted. The prediction of ground response is important in the development of the proposed area or area of interest since it reflects how the site can withstand potential external loads. In conducting GRa, input, such as time histories, soil data, and peak ground acceleration (PGa) for the proposed area, were required. Due to the fact that conducting soil investigations in offshore areas is very expensive and can be conducted by a related party, the data are some of the limitations of this study. Therefore, the selection of sites was based on soil data availability. Details on the time histories, soil data, and PGa were presented in the subsections.

2.1.1. Time Histories

In this study, time histories refer to the ground motion measurements due to seismic events, recorded by selected seismic stations in Malaysia. Seismic time histories were obtained from the Malaysian Meteorological Department (MMD). Six seismic events were selected for this study comprises of three near-fields (seismic events occurred in Malaysia) and three far-field (seismic events from Sumatera, Indonesia). The seismic events for far-field are Sumatera (25 July 2004), Sumatera (1 December 2006), and Sumatera (2 March 2016) known as F1, F2, and F3, respectively. Seismic events for near-field are Beluran, Sabah (23 May 2005), Kunak, Sabah (28 May 2012), and Ranau, Sabah (1 February 2014), noted as N1, N2, and N3, respectively. One of the criteria for the seismic time history selection is that the earthquake magnitude reach 5 or above for far-field seismic events (since lower values are considered as non-harmful to structures). Only secondary waves in the east–south (E) direction were used in this study with noise reduction due to the assumption that the recording station would capture all vibrations, including vibrations from surroundings other than the seismic. Figure 5 shows seismic time histories used in this study.

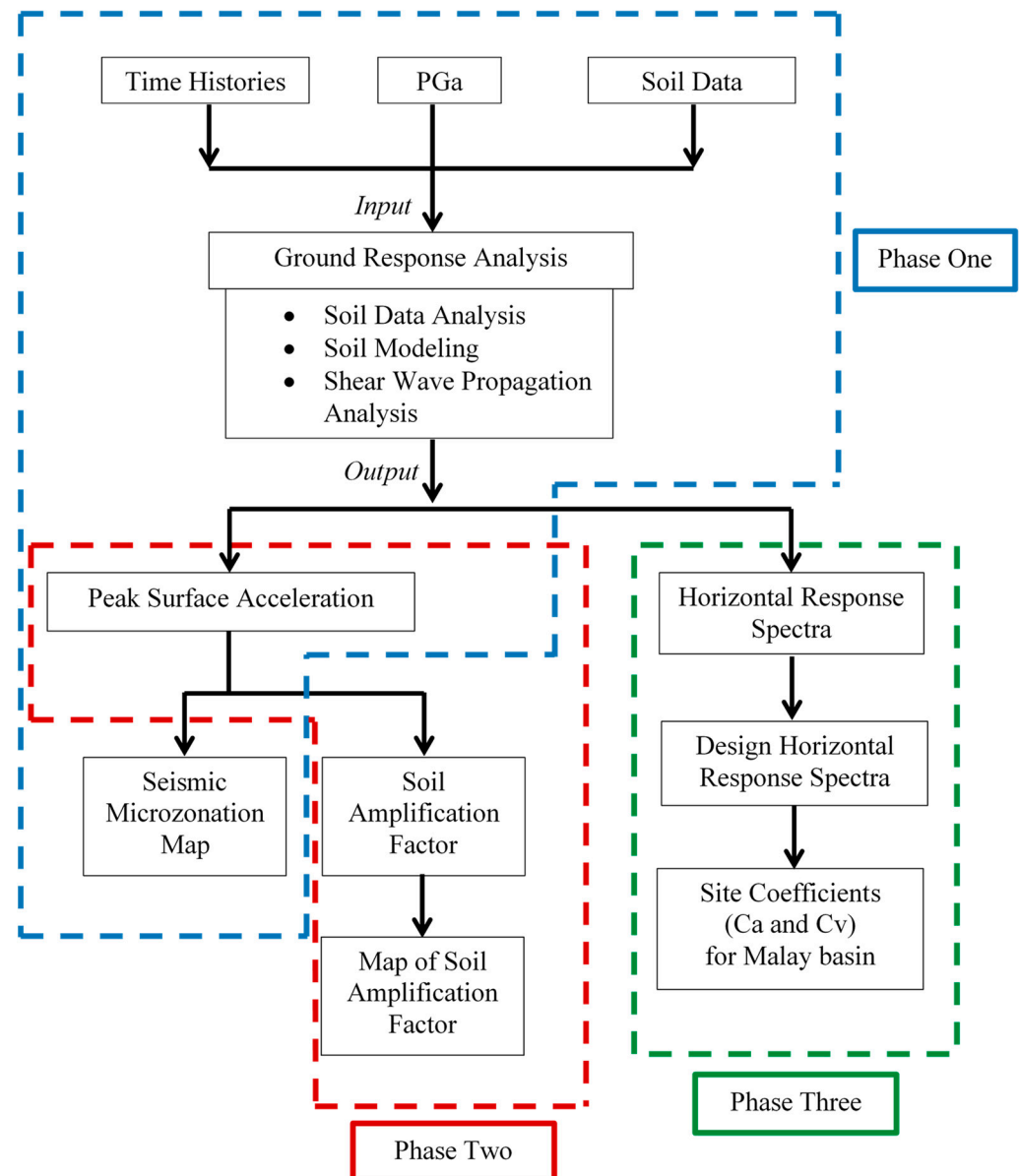


Figure 4. Flowchart of research methodology.

2.1.2. Soil Data

Conducting soil site investigations for offshore areas was very costly and required specialists. Furthermore, only related parties were involved and willing to undergo the process. Thus, limitations occurred in terms of data availability. Soil data in this study were extracted from a soil investigation report submitted to the related parties in the process of constructing the offshore platform. The report was based on the cone penetration test with pore pressure measurements (CPTU) conducted in the study area. The report consisted of data, such as coordinates, depth of the borehole, soil profile, number of soil layers, total unit weight, thickness of soil layers, and soil type. These data were required for GRa, including soil shear wave velocity. However, shear wave velocity is not available in the soil investigation reports. Thus, the determination of shear wave velocity through CPT-Vs correlation equations was required in solving this problem.

In the current study, six developed CPT-Vs correlations, which correlated Vs with the measured tip resistance (qc) and sleeve friction resistance (fs), and the correlation of Vs with qc only for the quaternary geological age, were selected. These correlation equations were developed based on soil types, such as sand, clay, and all soils [30–32]. In offshore

areas, normally the combination of clay and sand can be seen. CPT-Vs correlation equations adapted in this study are presented in Table 1. Values for soil shear wave velocities for each site were calculated by averaging the Vs from all soils and Vs calculated according to soil type. The same concept was applied by Hoe (2015) [33] in determining Vs for Malaysian offshore.

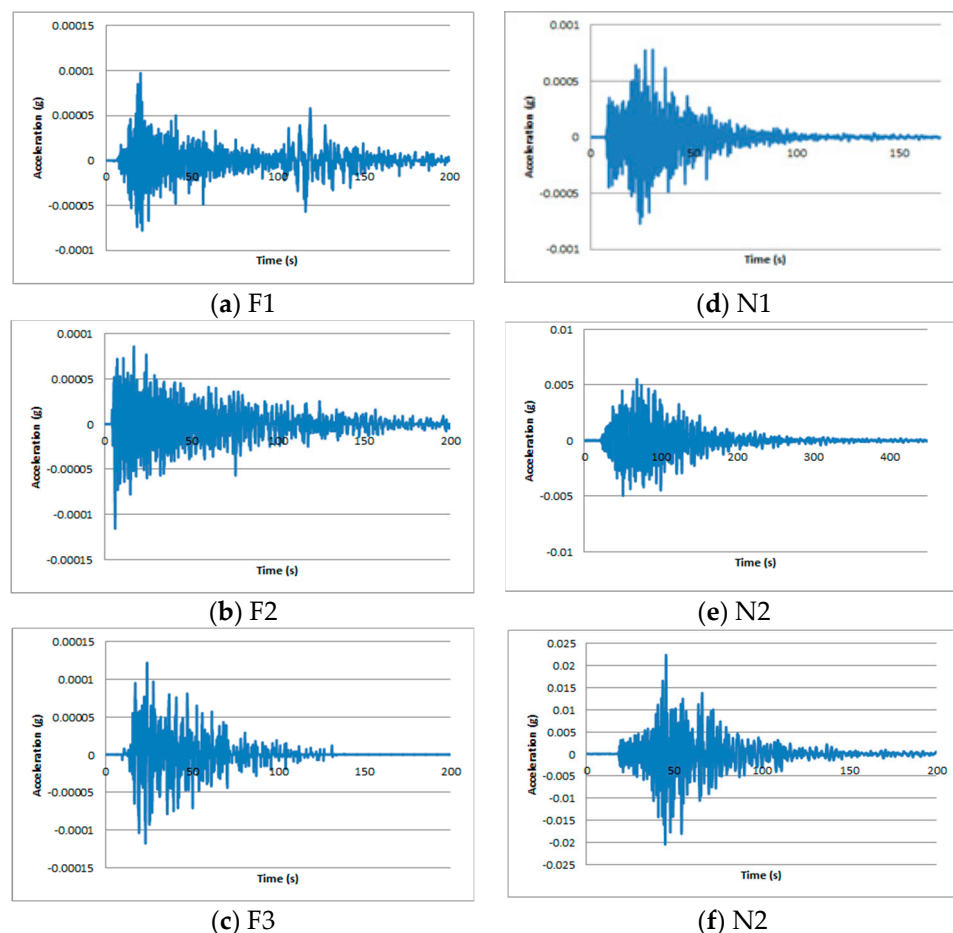


Figure 5. Seismic time histories.

Table 1. Correlation of CPT-Vs used in the present study.

Soil Type	Model	Equation for Vs	r ²	Paired Data
All Soil	Hegazy and Mayne (1995)	$(101 \log(q_c) - 11.4)^{1.47} (100 f_s / q_c)^{0.3}$	0.70	323
	Mayne (2007)	$118.8 \log(f_s) + 18.5$	0.82	161
Sand	Sykora and Stokoe (1983)	$134.1 + 0.0052 q_c$	0.61	256
	Hegazy and Mayne (1995)	$12.02 q_c^{0.319} f_s^{-0.0466}$	0.57	92
Clay	Hegazy and Mayne (1995)	$3.18 q_c^{0.549} f_s^{0.025}$	0.78	229
	Mayne and Rix (1995)	$1.75 q_c^{0.627}$	0.74	481

After the data collection and screening process, there were 11 sites available with a total of 19 boreholes data. These sites were then classified according to soil type as suggested in ISO 19901-2. In the current study, the soils were classified according to the Vs of the first 30 m that were calculated using Equation (1). From the 11 sites, 4 were sited under soil type D and 7 under soil type E. Thus, D1–D4 represent sites for soil type D and E1–E7 represent sites for soil type E. The letter D represents soil type D and E represents soil type E while the number represents the numbering for the site. A sample of the soil model used in the present study is presented in Table 2.

Table 2. Soil model for D1 used in the present study.

Depth (m)		Thickness	Soil	Vs
From	To	(m)	Description	(m/s)
0.0	6.9	6.9	Very soft to soft clay	117.764
6.9	9.8	2.9	Stiff silt	193.169
9.8	14.9	5.1	Stiff clay	162.077
14.9	21.6	6.7	Firm to stiff clay	150.722
21.6	24.0	2.4	Very stiff silt	282.296
24.0	27.2	3.2	Firm clay	208.693
27.2	29.8	2.6	Very stiff silt	231.147
29.8	38.9	9.1	Stiff clay	200.705
38.9	44.8	5.9	Stiff to very stiff clay	204.381
44.8	50.0	5.2	Very stiff silt	280.731

2.1.3. Peak Ground Acceleration (PGa)

Peak ground acceleration (PGa) is the prediction of the amount of vibration received by any specified site or location. In this study, the PGa input was extracted from a previous study [34]. PGa values obtained from this study were extracted from these findings for 100-year, 200-year, 500-year, 1000-year, and 2500-year return periods based on the site locations. The PGa values used in the current study (extracted from a previous study) are presented in Table 3.

Table 3. PGa values for offshore Peninsular Malaysia [34].

Coordinate		PGa (g)				
Lat.	Long.	100-Year Return Period	200-Year Return Period	500-Year Return Period	1000-Year Return Period	2500-Year Return Period
3.0	103.5	0.02	0.03	0.04	0.05	0.07
3.5	103.5	0.02	0.03	0.03	0.05	0.07
4.0	103.5	0.02	0.02	0.03	0.04	0.06
4.5	103.5	0.02	0.02	0.03	0.04	0.05
5.0	103.5	0.02	0.02	0.03	0.03	0.05
5.5	103.5	0.02	0.02	0.02	0.03	0.04

2.1.4. Ground Response Analysis (GRa)

In this study, one-dimensional nonlinear analyses were carried out by using the Nonlinear Earthquake Site Response Analysis of Layered Deposits (NERA) program. GRa in this study was conducted for 11 sites with a total of 19 boreholes for 6 seismic events and 5 return periods. The overall methodology for GRa is depicted in Figure 4. In NERA, the first step is to decide the time step increment, desired maximum acceleration, and maximum frequency cut-off. In the current study, the time step increment was set to 0.01 while the desired maximum acceleration was set to ensure that the PGa value at the bedrock reflected the value. The maximum frequency cut-off was set at 10 Hz. All of this information is the input in the worksheet 'earthquake'. Along with that, the selected seismic time history was inserted.

The second step was to provide the soil parameters in the worksheet 'profile'. However, soil material type, thickness of a layer, total unit weight, and shear wave velocity were added. A sample of worksheet profiles is presented in Table 4. There were 2 soil material types available, '1' represents clay while '2' represents sand [35]. The number of time-sub increments in the worksheet 'Iteration' was set at the minimum value and the outcrop was set for the type of input motion. In the worksheet 'Spectra', a number of sublayers were set as 1 to represent the surface or seabed while the ratio of critical damping was set at 5%, as suggested in the ISO19901-2 [26].

Table 4. Worksheet Profile in NERA for D1 site.

Fundamental Period (s) = 1.04 Average Shear Wave Velocity (m/sec) = 192.95 Total Number of Sublayers = 11									
	Layer Number	Soil Material Type	Thickness of Layer (m)	Maximum Shear Modulus G_{max} (MPa)	Total Unit Weight (kN/m ³)	Shear Wave Velocity (m/sec)	Location of Water Table	Depth at Top of Layer (m)	Vertical Effective Stress (kPa)
Surface	1	1	6.9	25.49	18.03	117.764		0.0	0.00
	2	1	2.9	68.58	18.03	193.169		6.9	124.41
	3	1	5.1	48.28	18.03	162.077		9.8	176.69
	4	1	6.7	41.75	18.03	150.722		14.9	268.65
	5	1	2.4	168.40	20.73	282.296		21.6	389.45
	6	1	3.2	85.82	19.33	208.693		24.0	439.20
	7	1	2.6	105.28	19.33	231.147		27.2	501.06
	8	1	9.1	79.37	19.33	200.705		29.8	551.31
	9	1	5.9	76.77	18.03	204.381		38.9	727.22
	10	1	5.2	155.29	19.33	280.731		44.8	833.59
Bedrock	11	0		3333.52	22.00	1219.2		50.0	934.11

After everything was assigned, the first step was to use the process earthquake data command where, here, the time history input was processed to achieve the desired PGA value. The second step was executed by using the ‘calculate’ step-by-step command; in this stage it involved the NERA read profile, material curve, and then the execute the key calculation to produce the acceleration, velocity, and displacement in the worksheet ‘Iteration’. The third step was to produce the output by using the command ‘Calculate Output’. In this stage, the output for spectra in terms of acceleration was obtained. The maximum acceleration at sublayer 1, produced in the Iteration worksheet, was recorded as it portrayed the value of the acceleration at the seabed or surface. The movements of the wave propagation in vertical motion throughout the soil layers and the spectra for the surface were produced.

2.1.5. Plotting Seismic Microzonation Map

The last stage in phase one was to plot a seismic microzonation map for each site according to the return period. As discussed earlier, there are five return periods used in this study, consisting of 100-year, 200-year, 500-year, 1000-year, and 2500-year return periods. Seismic microzonation map-plotting was performed by using ArcGIS software. The inverse distance weighted (IDW) tool was used to create the contour of PSa for this study according to the return period. The estimation of a new point was made by averaging the values of data that were close to the processing cell.

The process of plotting the seismic microzonation map started with creating a new template in ArcMap. Then, a layer of the map was added, which portrayed the map of Malaysia before continuing with adding a Microsoft table in ArcMap as the input data; for this case, input data consisted of coordinates and PSa values. Since the data were in an excel file, the data for the x axis and y axis were imported to ArcMap by using add XY data. A shapefile was created to ease the editing process during data editing. The digitizing process is a process where the boundaries of PSa maps are digitized. The data were created as coordinates in polygon format. Moreover, the coordinate system used was GCS WGS 1984 for the geographic coordinate system. This boundary was used to limit the area where the contour was plotted.

To create a contour, a model builder was used. The model was the workflow arranged to allow processing of the input data by incorporating geoprocessing tools to produce an output, which then could be used as the input for another tool. In this study, PSa was used as the input, and the contour was created using inverse distance weighted (IDW). IDW is one of the raster interpolation toolset available in Spatial Analyst Tools under geoprocessing. Since IDW uses an interpolation technique, it only can predict the point in the range of the dataset. Plotting of the contour was performed using Contour, one

of the raster surface toolsets in Spatial Analyst Tools, available in ArcToolbox or the 3D analyst toolbox.

2.2. Phase Two: Development of Map for Soil Amplification Factor

Phase two was designed to achieve the second objective in this study, which was to develop a map of soil amplification factors for the Malay Basin. A map for soil amplification factors was developed based on the soil amplification factor calculated for the study areas. From ground response analyses, results of the peak surface acceleration (PSa) for study areas were obtained. These values were used to determine the soil amplification factor by using Equation (2).

$$\text{Soil Amplification Factor} = \frac{\text{PSa}}{\text{PGa}} \quad (2)$$

Results of the soil amplification factor (AF) for each site were calculated for 100-year, 200-year, 500-year, 1000-year, and 2500-year return period under six seismic events. A comparison of results was carried out for far-field and near-field seismic events. Then, the results were averaged over seismic events to avoid underestimating and overestimating the seismic effects. The average results were used to produce five soil AF maps representing each return period. These values along with the coordinates were among the main input in ArcGIS software for map-plotting, ArcMap. The inverse distance weighted (IDW) method was used where the interpolation theory was adapted in predicting new values for soil AF based on nearby points. Contour, one of the raster surface toolsets under Spatial Analyst Tools, was used to plot the AF maps. The same coordinate system and grid as in Section 2.1.5 were used in creating and plotting the maps.

2.3. Phase Three: Determination of Site Coefficients and Design Horizontal Response Spectra

Phase three was designed to achieve the third objective of this study. In this phase, the response spectra, which were obtained from the ground response analysis, were analyzed to determine the designed horizontal response spectral acceleration. The curves and spikes in the horizontal response spectra were smoothed by proposing a single line known as designed horizontal response spectral acceleration (DHRSa). For response spectra, only results of the 1000-year return periods were used, and the damping was assumed to be 5%. The spectral acceleration (Sa) values of the 1000-year return period for 0.2 s and 1.0 s were extracted from a previous study [34]. Details of the site coefficients and designed horizontal response spectra in acceleration are presented herein.

The process of proposing DHRSa started with analyzing horizontal spectral acceleration output from GRa conducted using NERA, a one-dimensional nonlinear ground response analysis. Horizontal response spectra for each site were analyzed according to seismic events and sites, then the results were plotted for spectral acceleration versus the period. Comparisons of the horizontal spectral accelerations were made to determine the effects of far-field and near-field and a combination of far-field and near-field seismic events. Then, plotting of horizontal response spectra for the average as well as the envelope was made based on soil type. After that, comparisons were made between horizontal response spectral accelerations obtained with the proposed horizontal response spectra by ISO19901-2 [26]. A sample of the horizontal response spectra for site D4 is presented in Figure 6 for far-field seismic events. The same analysis was conducted for all sites. The average of each site was used to obtain the average and envelope for soil types D and E. From the plotting, the constant acceleration value was selected and used in the process of proposing the site coefficient for acceleration (Ca) and site coefficient for velocity (Cv).

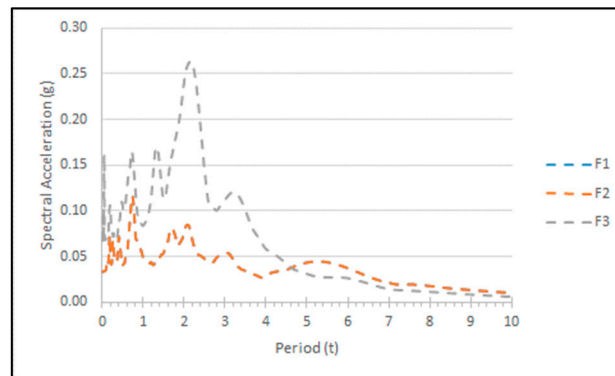


Figure 6. Sample of the spectral acceleration for D4 under far-field seismic events.

The C_a and C_v values are important in the construction of horizontal response spectra in acceleration. The values of the proposed C_a and C_v in this study were calculated by implementing back-calculations of the equation suggested in ISO19901-2. The equations used in the construction of DHRSa can be seen in Equation (3) to Equation (6). Equation (3) is used when T (natural period) is less or equal to 0.2 s while Equation (4) is for T greater than 0.2 s but less than 4 s if only the S_a for that site follows the condition in Equation (5). Equation (6) is used when the period is greater than 4 s but less than 10 s. To calculate the site coefficients, the values of S_a at 0.2 s and 1.0 s periods must be known. In this study, the values were extracted from a previous study [34] where a probabilistic seismic hazard assessment was conducted to predict the value. The S_a values and values of C_a and C_v proposed by ISO19901-2 were used in this study. The S_a map for 0.2 s was 0.05 and the S_a map for 1 s was 0.02. For soil type D, C_a was 1.6 and C_v was 2.4, while in soil type E, C_a was 2.5 and C_v was 3.5.

$$S_{a, site}(T) = (3T + 0.4)C_a \times S_{a, map}(0.2) \quad (3)$$

$$S_{a, site}(T) = C_v \times S_{a, map}(1.0) / T \quad (4)$$

$$S_{a, site}(T) \leq C_a \times S_{a, map}(0.2) \quad (5)$$

$$S_{a, site}(T) = 4C_v \times S_{a, map}(1.0) / T^2 \quad (6)$$

where;

T is the natural period;

C_a, C_v are the site coefficients;

$S_{a, site}(T)$ is the site spectral acceleration corresponding to period T ;

$S_{a, map}(0.2)$ is the site spectral acceleration corresponding to period 0.2 s;

$S_{a, map}(1.0)$ is the site spectral acceleration corresponding to period 1.0 s.

Site coefficients and C_a – C_v values proposed in this study were calculated by setting the maximum S_a value at 0.2 s based on the plotted HRSa. The C_a value was calculated using Equation (5). The period where the constant acceleration end was selected, and the T value was used to calculate C_v . In this study, the C_v value was calculated by equating Equation (4) with Equation (5). Once C_a and C_v values were obtained, the proposed DHRSa for each soil type could be plotted. This DHRSa was proposed for soil types D and E only, in accordance with the condition provided in ISO19901-2 [26]. DHRSa was proposed for the average and envelope of far-field, near-field, and a combination of far-field and near-field. A comparison of the proposed DHRSa with ISO19901-2 for each condition was made and the results are presented in the figures.

3. Results and Discussion

This section highlights the results obtained in the seismic microzonation map for a fixed-jacket platform in the Malay Basin. The three objectives in this study are presented in

three main phases—developing a seismic microzonation map, developing a map of the soil amplification factor, and proposing a designed horizontal response spectral acceleration and site coefficient for the study area. Details for each phase are presented in Sections 3.1–3.3. Please note that the labeling of results was based on the site and soil type at that site. For soil type D, there were four sites, known as D1, D2, D3, and D4. As for soil type E, there were seven sites, known as E1, E2, E3, E4, E5, E6, and E7. As an example, D1 refers to the first site for soil type D.

3.1. Development of Seismic Microzonation Map

This phase underlines the first objective, which was to develop a seismic microzonation map for the Malay Basin. Since this was a large scope to cover, two sub-objectives were introduced—determination of the peak surface acceleration and plotting the seismic microzonation map. Details on each sub-objective are presented in the following subsections.

3.1.1. Determination of Peak Surface Acceleration

Peak surface acceleration (PSa) is the amount of vibration received by the soil surface; in this study, it refers to the seabed. It is the results of the ground response analysis conducted for the study area. As discussed in a previous section, a non-linear ground response analysis for the one-dimensional analysis, namely NERA, was adopted in this study. Six (6) seismic events were used, three events from Sumatera and three events from Sabah varies from 2004 to 2016. PSa were obtained for five (5) different return periods (100-year, 200-year, 500-year, 1000-year, and 2500-year return periods). In this sub-section, the sample of PSa results is presented for far-field soil type D. Thus, the effects of different sites can be viewed.

The results presented in this section are based on GRa conducted where the value of PGa was obtained from the bottom point of the last layer of the soil in the analysis, which was considered as the bedrock, while PSa was the value of the vibration in the acceleration predicted on the first layer, which was the surface (known as the seabed in this study). The result for PSa was taken from the acceleration value on the first layer. In the sample, PGa and PSa were analyzed by providing the mean according to far-field. Figure 7 presents PGa and PSa for soil type D. Figure 7a represents the PGa and PSa values for site D1 where the minimum PGa was 0.02 g at the 100-year and 200-year return periods while the maximum value was 0.05 g at the 2500-year return period. Referring to Figure 7b, the results of PGa and PSa for site D2 can be seen. The PGa value is within 0.02 and 0.05 g while for the PSa value, a slight increment can be seen for all return periods except for the 100-year and 200-year return periods when compared with site D1. The predictions of PSa values range from 0.03 to 0.057 g. Lower PSa values can be seen when the site comprises stiffer soil.

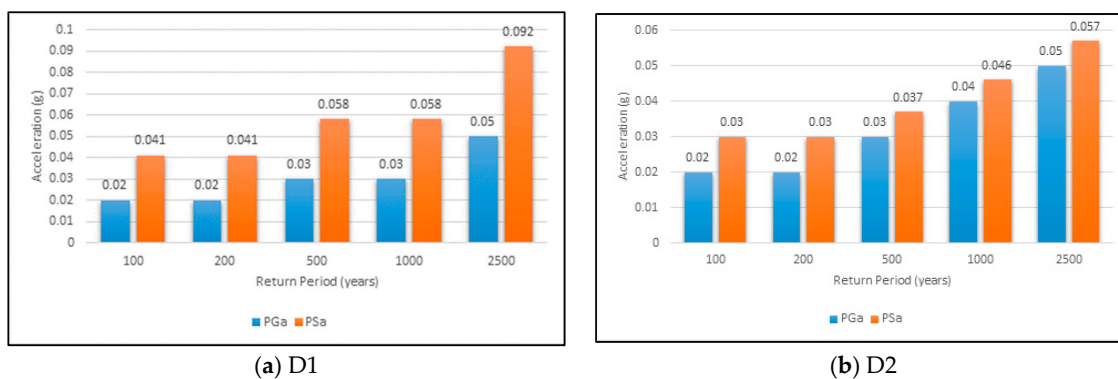


Figure 7. PGa and PSa for D1 and D2 under far-field seismic events.

Overall, GRa was conducted in the prediction of vibration received by surface or seabed by using NERA where six seismic events were replicated to predict the amount of the vibration on the surface. Based on seismic events, PSa for far-field was lower compared to a combination of far-field and near-field events, and near-field events. A comparison

of the soil types resulted in soil type D being lower compared to soil type E. Hence, the average PSa from a combination of far-field and near-field seismic events was used in developing a map for the Malay Basin under seismic microzonation. Results found in this study align with previous studies where seismic events from the far-field were found to produce smaller ground acceleration but in a longer period compared to near-field seismic events [20,36,37]. A higher value was found in higher return periods, such as 1000-year and 2500-year return periods. The same pattern was found by other researchers [20,21,38].

3.1.2. Plotting Seismic Microzonation Map

In this section, five seismic microzonation maps were plotted covering 100-year, 200-year, 500-year, 1000-year, and 2500-year return periods for PMO. The values of the average PSa were used to plot the map. PSa here is the prediction of the amount of the vibration at the seabed in terms of acceleration. Please note that seismic microzonation in this study refers to the inclusion of the local soil effect in the macrozonation study as discussed in the introduction section. Figures 8 and 9 show seismic microzonation maps plotted for the Malay Basin. A detailed map is shown in Figure 8 while Figure 9 presents a seismic microzonation map for the square area in Figure 8 under five return periods. Referring to Figure 9, higher values of acceleration can be seen compared to the macrozonation map provided in the standard [26], where the influence of soil layers during vertical motion was ignored. The amount of vibration was found to be higher with the wave traveling in a vertical motion, especially when there was a thick-soft soil layer. Overall, only 100-year and 200-year return periods shared the same pattern. This was due to PGa values for 100-year and 200-year return periods being mostly the same value. Since PSa was predicted from the PGa value plus the inclusion of soil layers up to the seabed, the value provided in PGa will definitely affect the PSa value. The PSa values in the maps showed incremental trends as the return period increased. This is supported by Carlton et al. (2022) [39], where a comparison of PGa values based on return periods showed a linear correlation (where a higher value was obtained for a higher return period).

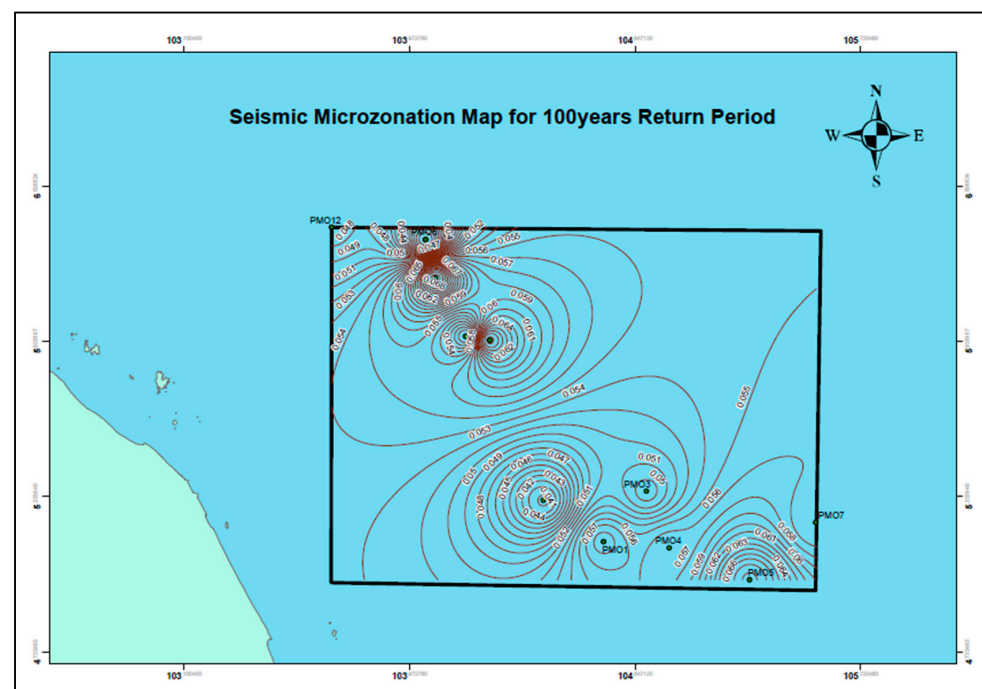


Figure 8. Seismic microzonation map for a 100-year return period.

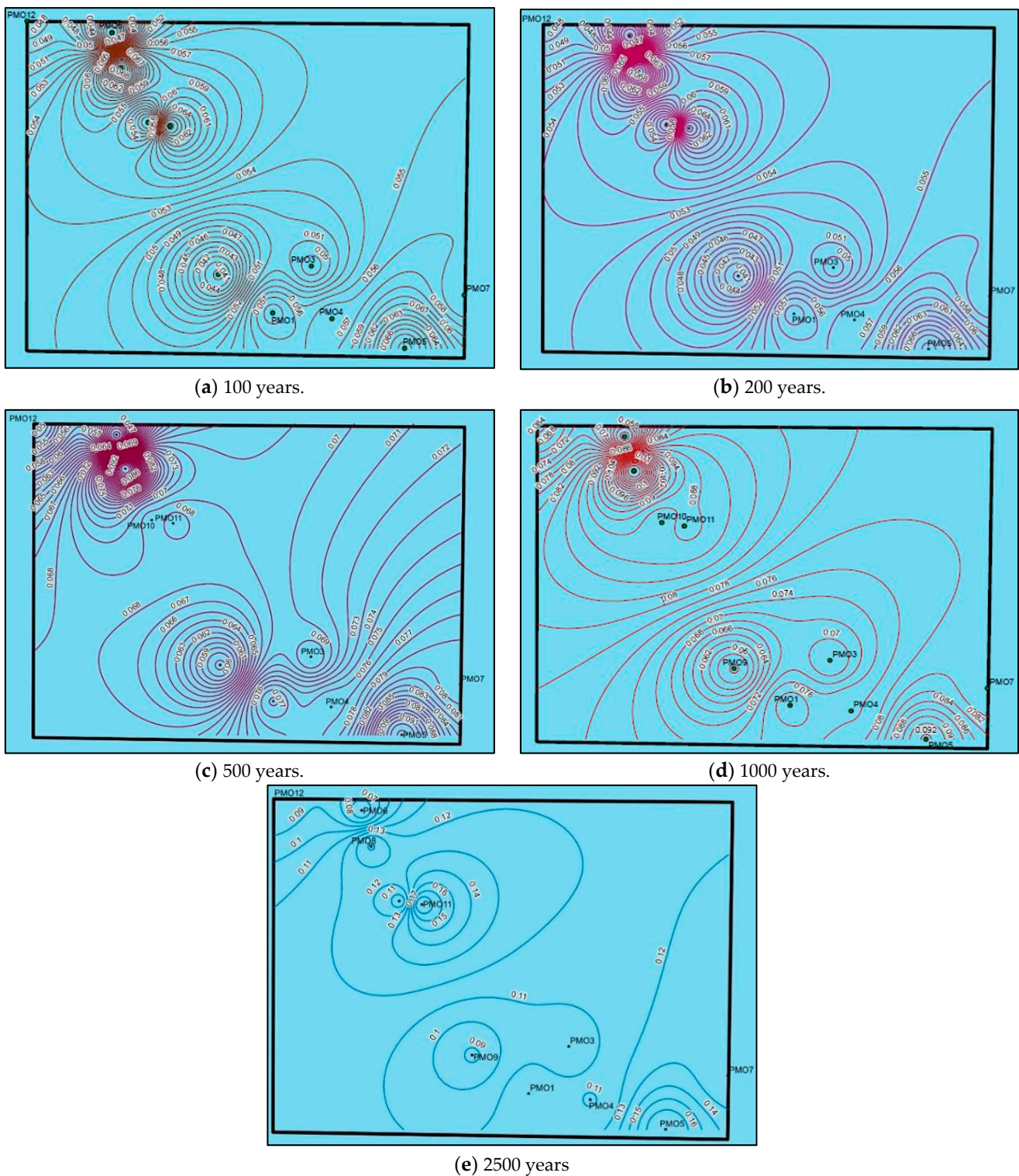


Figure 9. Seismic microzonation map for five return periods.

Birkmann (2013) [40] suggested that maps and figures representing characteristics of the complex phenomenon should be used as communication tools for the hazard. Hence, in the current study, the seismic microzonation map for the Malay Basin was proposed to ‘ease’ non-experts, the general public, and policymakers—to help them understand the potential hazards due to vibration before seismic events. This map can be used as one of the guidelines in the design process and risk assessment for maintenance purposes.

3.2. Development of Map for Soil Amplification Factor

This phase covers the determination of the soil amplification factor and map-plotting for the selected sites under six seismic events for five return periods. The existence of soil amplification at any location is affected by a combination of soil layers in terms of soil type and thickness. It is known that offshore areas normally consist of soft soil that has high potential in experiencing an amplification effect. In the Malay Basin, many offshore facilities are already aging but are still operating; this type of structure has potential in experiencing additional lateral loads if an amplification effect exists. However, the existence of the amplification effect in the Malay Basin is still questionable. Thus, the second objective of this study was to develop a map of soil amplification factors for the Malay Basin. The soil amplification factor presented in this phase could be used in the analysis after obtaining PGa values of any location, which was predicted using the attenuation equation.

3.2.1. Determination of Soil Amplification Factor

Soil amplification is calculated by using Equation (2) and it represents the increment of vibration as it travels upward through layers of soil at any location. In this study, the amount of vibration at the surface is represented by Psa while the amount of vibration on the bedrock is called Pga. Any specified location experienced amplification if the amplification factor is more than 1.0. Results of soil amplification factors for soil types D and E for far-field seismic events can be seen in Figure 10, as a sample of the analysis conducted. The soil amplification factors for each site were presented according to the return periods. The red line in the figures represents the boundary to show that amplification occurs if the value passes that red line. Soil type D is stiffer compared to soil type E and each site has its combination of soil layers in terms of thickness for each layer and type of soil, either clay or sand. Overall, it can be concluded that the values of soil amplification factors for soil type D are lower compared to soil type E for both far-field and near-field. When comparisons were made between far-field and near-field, the site underwent near-field seismic events that produced higher soil amplification. Thus, soil amplification is affected by the intensity of the seismic event, distance of the site to the epicenter, and the soil layers beneath the seabed. Hence, soil amplification predicted in this study was limited to the study area only.

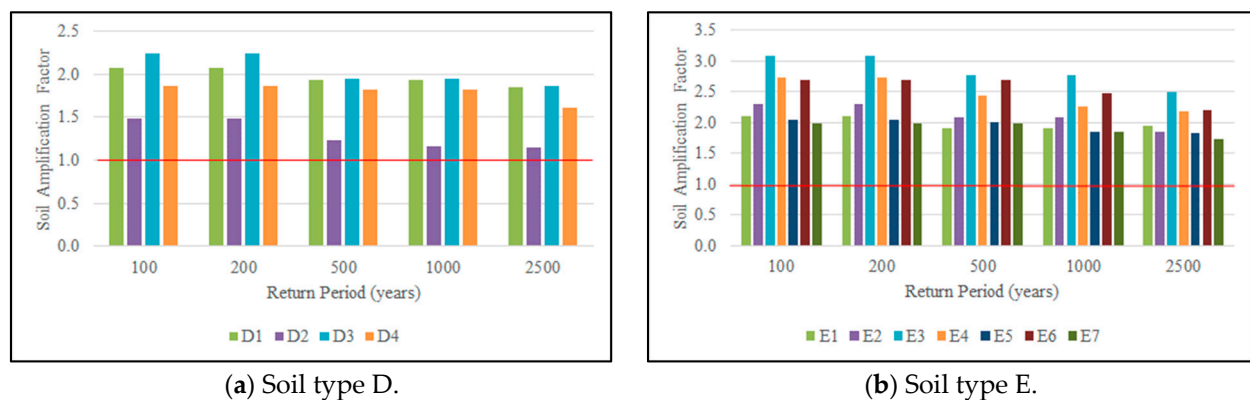


Figure 10. Soil amplification factor for soil types D and E under far-field seismic events.

3.2.2. Plotting Map of Soil Amplification Factor

Before the seismic microzonation map, a map for the soil amplification factor (AF) was plotted to ease the related parties in obtaining an overview of the AF prediction at the Malay Basin. Figure 11 portrayed a complete map for the soil AF and the scale and showing map of the soil AF for the 100-year return period. The black square on the map represents the study area. The soil AF contour maps of this study area, according to the five return periods, can be seen in Figure 12. These maps were plotted by using ArcGIS software by implementing the IDW method. These maps consist of soil types D and E. Values of the soil AFs predicted in the map can be used to predict the amount of soil amplification in the

study area to determine the reliability of the existing structure or to design a new structure in the study area.

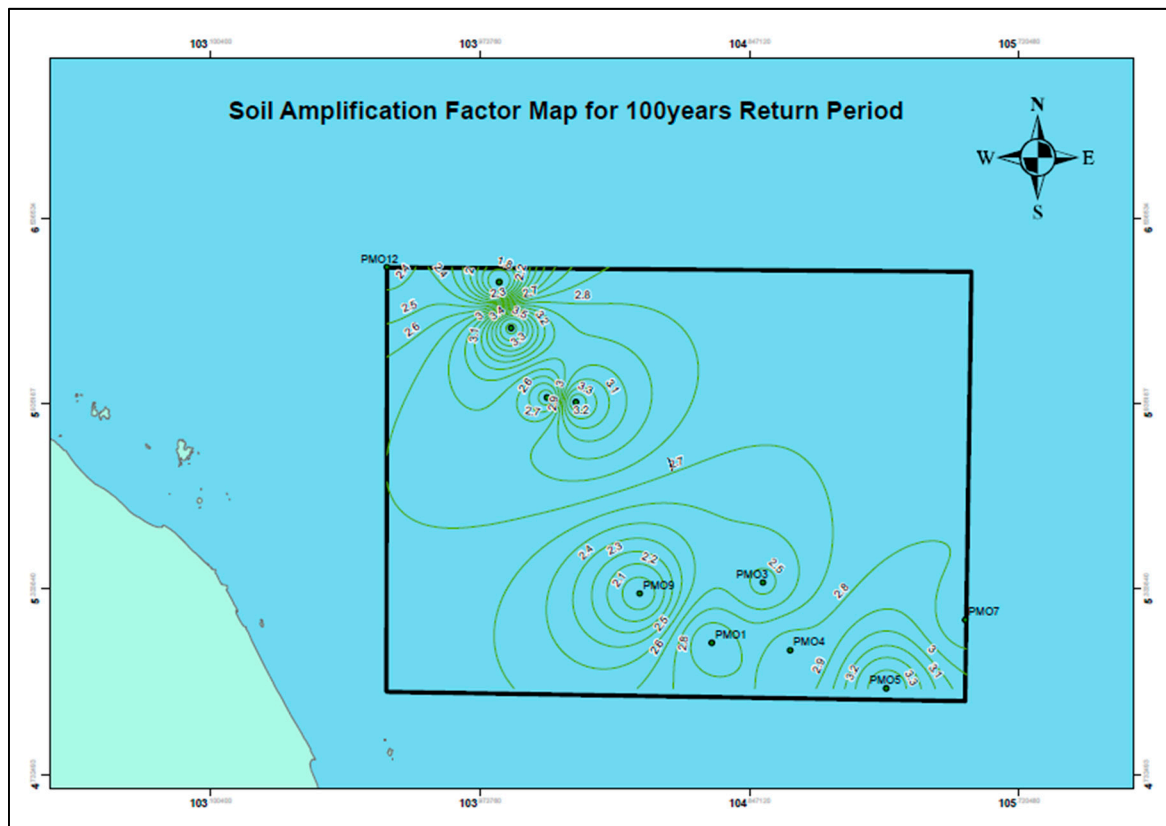


Figure 11. Map of the soil amplification factor for the 100-year return period.

Referring to Figure 12, results show that the soil amplification factor decreased as the return period increased. Soil type E obtained the soil amplification factor, which was higher than soil type D. The same pattern can be found in Nabilah et al. (2017) [37]; the lowest soil class used in the study consisted of clay soil, with a higher plasticity index producing the highest soil amplification factor of 4.5. The higher amplification is suggested to occur when the seismic and soil frequency coincide. Thitimakorn and Raenak, (2016) [41] obtained soil amplification factors between 1.4 and 2.8 for a site in Northern Thailand. It was suggested that this happened due to site geological conditions where the thickness of the sediment for this area was relatively thin and there was bedrock underlying this part of Lamphun city. Firat et al. (2015) [23] agreed with this scenario, as soil conditions and local sites can influence the soil amplification (this was experienced in the Adapazari region before the Kocaeli earthquake in 1999). Furthermore, Yunita et al. (2018) [42] found soil amplification factors for Banda Aceh, which is underlain by soft soil up to 4.3. Thus, the soil amplification factor should be used to estimate the amount of vibration received by the ground surface when a seismic event occurs.

3.3. Determination of Design Horizontal Response Spectra and Site Coefficient

In this phase, results on the design horizontal response spectral acceleration (DHRSa) and proposed site coefficients were presented. The DHRSa proposed in this study was based on six seismic events on the selected sites (D1–D4, E1–E7) consisting of soil types D and E based on ISO 19901-2 classification. The results were gained from GRa conducted using NERA, a one-dimensional nonlinear ground response analysis. This phase presents results for the third objective of this study—proposing designed horizontal response spectra and site coefficient values (C_a and C_v) for the Malay Basin. The DHRSa was proposed for

far-field, near-field, and a combination of far-field and near-field. Results of the average and envelope for each soil type were compared with DHRSa, predicted by ISO 19901-2.

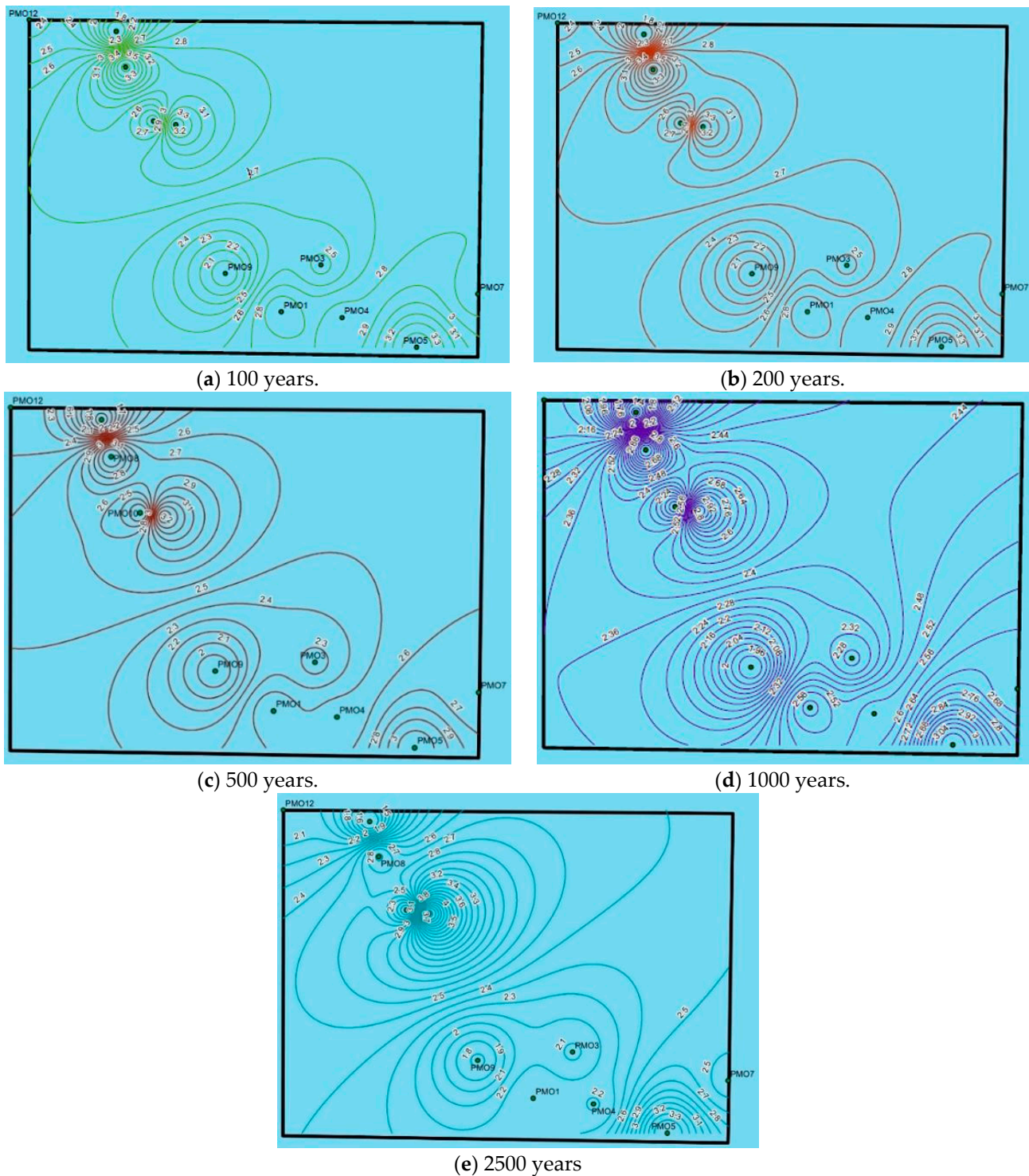


Figure 12. Map of the soil amplification factor for the 200-year return period.

3.3.1. Design Horizontal Response Spectra

In this study, results of spectral acceleration were presented based on far-field, near-field, and a combination of far-field and near-field. Then, DHRS were proposed based on the average and envelope for soil types D and E. Far-field seismic events were represented by F1–F3, while near-field seismic events were represented by N1–N3. Results of the

average spectral acceleration under far-field seismic events obtained from one-dimensional nonlinear GRA for sites D1–D4 under far-field, near-field, and a combination, are presented in Figure 13. This phase proposes DHRSa for soil types D and E. However, only results for soil type D are discussed in this section to help in understanding the process of proposing DHRSa.

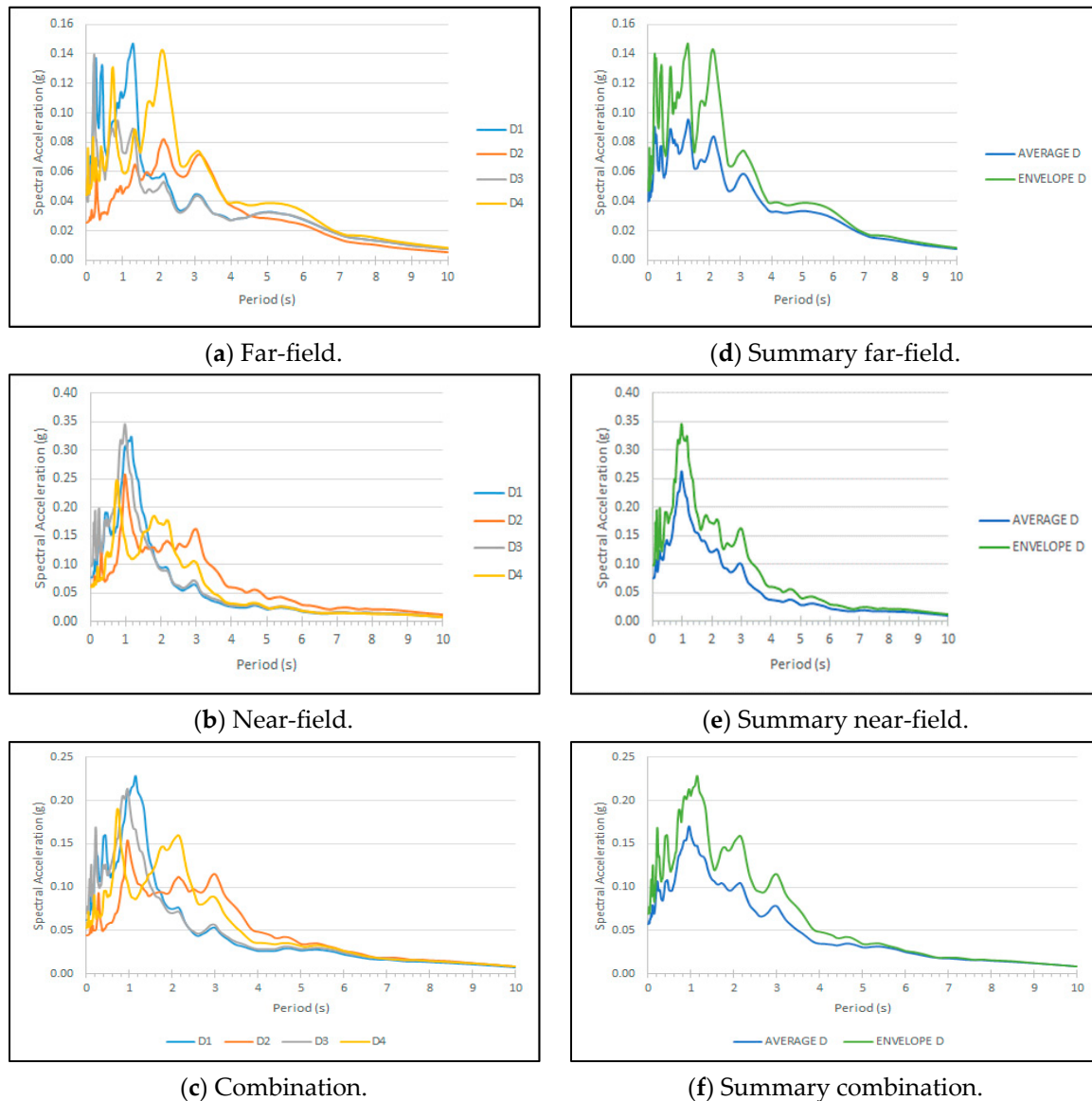


Figure 13. Average spectral acceleration for soil type D.

Referring to Figure 13a, it can be seen that three out of four sites in this study showed a peak value of approximately 0.14 g. Site D3 showed a peak value at 0.2 s while at site D1, the peak value occurred between 1 and 2 s. At sites D2 and D4, the peak values occurred between 2 and 3 s. In far-field seismic events, highest Sa values were predicted for F3; in all events, D2 showed the lowest value. The average and envelope for each site were then used in predicting Sa for soil type D under far-field seismic events, as shown in Figure 13d. The highest peak for the average was 0.90 g, which occurred at 1.35 s while the highest value for the envelope was 0.146 g at 1.3 s.

Figure 13b,e show results on DHRSa under near-field seismic events for soil types D and E. Three seismic events were used in the analysis of the ground response of the selected sites in the Malay Basin. In Figure 13b, the peak for D3 was slightly higher than D1 while D2 was slightly higher than D4. The highest value predicted at D3 was almost

0.35 g. The lowest value for the peak was found at site D4, which was close to 0.25 g. To avoid underestimating or overestimating, the average of all seismic events along with the envelope of HRSa for soil type D, are plotted in Figure 13e.

After looking at the Sa based on the single application of either far-field or near-field, results of Sa for each site were combined and the average (based on soil type) was plotted. The plotting of the average soil type D under the combination of far-field and near-field is shown in Figure 13c. The highest peak occurred at D1, followed by D3, D4, and D2. D1 and D3 shared a slightly different pattern of Sa over a period. The average and envelope of Sa for D1–D4 are plotted in Figure 13f. The highest value for the average was 0.17 g and 0.23 g for the envelope of soil type D. The peak motion at sites D1 until D4 occurred around 1 s.

Results for the proposed DHRSa along with Sa proposed by ISO 19902 were compiled (Figure 14a,b) based on soil type. From Figure 14a, the proposed DHRSa for soil type D were higher compared to DHRSa proposed in ISO 19902, except for Dave far-field which was slightly higher by 0.004 g. In terms of region, for constant acceleration in DHRSa, the proposed DHRSa obtained longer periods compared to ISO. Dave near-field recorded the same highest Sa value as the Denv combination but with a shorter period of constant acceleration. Looking into the seismic scenario (far-field, near-field, and the combination), the Dave far-field had the lowest value while the Denv near-field produced the largest value. In Figure 14b, it can be seen that the average and envelope of the proposed DHRSa were also higher compared to ISO. The longest constant acceleration period occurred in the far-field, followed by near-field and the combination. A comparison in the constant acceleration region resulted in a shorter period for ISO compared to the proposed DHRSa.

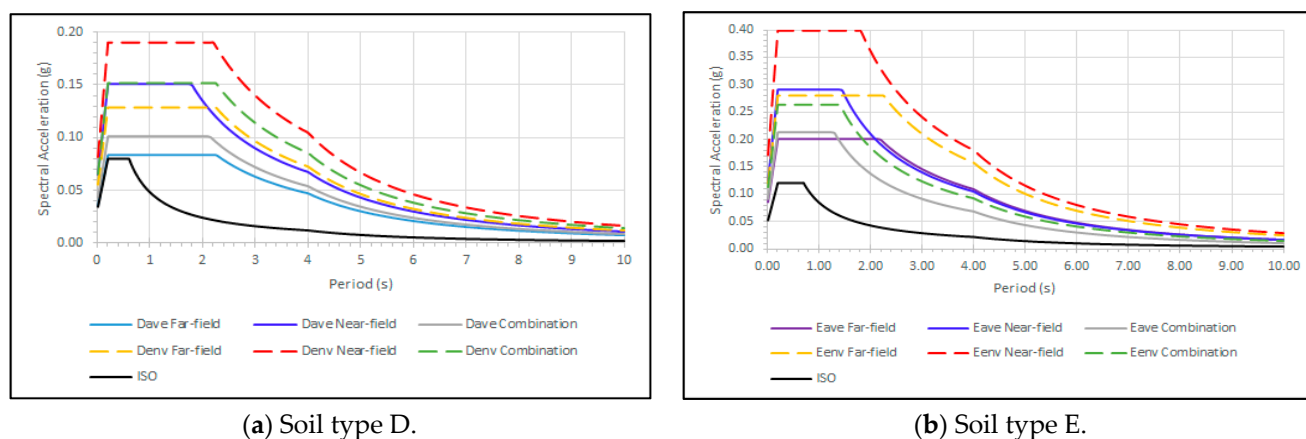


Figure 14. Comparison of DHRSa and ISO for soil types D and E.

In this section, DHRSa under a 5% damping ratio for the 1000-year return period and site coefficient values for the Malay Basin are proposed. The design horizontal response spectral acceleration was proposed for the average and envelope under three seismic conditions—near-field, far-field, and a combination of near-field and far-field seismic events. This eased the related parties to decide which scenario best fit the site condition. Based on the results, it was found that soil type D had a lower value compared to soil type E. The same findings can be seen in work by Majid et al. (2007) [43], where soil type E produced higher spectral acceleration compared to stiffer soil, such as soil type D. It was suggested that response spectral acceleration is strongly related to soil parameters, the depth of soil, and PGa. Asakereh et al. (2015) [44] stressed that the response spectra due to different seismic events (but having the same input acceleration) would be different due to different frequency content. It should be noted that both maximum acceleration and frequency content must not be higher than standard response spectra used in the construction of the structure because it will be severely damaged.

In the current study, far-field seismic events produced longer periods of constant acceleration compared to near-field. This is supported by previous researchers, who found

the same patterns in their studies [20,45]. In both soil types, all conditions showed higher design horizontal response spectral acceleration except for the average of far-field for soil type D. In Dave far-field, the spectral acceleration was slightly higher, but the constant acceleration period was higher.

3.3.2. Site Coefficients for Acceleration and Velocity (C_a and C_v)

When dealing with a shallow foundation, Site coefficients known as C_a and C_v values are dependent on the site; S_a was predicted for 0.2 s and 1.0 s periods [26,28]. The response spectrum analysis was found to be an effective linear analysis and cost-effective when dealing with the seismic analysis [28]. $DHRS_a$ can be presented in the form of a graph, or it can also be plotted based on equations proposed by ISO19901-2 if the values of C_a and C_v are available. The third objective of this study was to propose C_a and C_v values of soil types D and E for the Malay Basin. The proposed C_a and C_v values for this study, along with proposed values by ISO19901-2, are presented in Table 5.

Table 5. Comparison of the proposed C_a and C_v values with ISO19901-2.

	Type of		Site Coefficient		
	Seismic Events	DHRSa	Soil Type	C_a	C_v
PROPOSED	Far-field	Average	D	1.5	3.7
		Envelope		2.5	6.0
		Average	E	3.6	9.2
		Envelope		4.5	11.8
	Near-field	Average	D	2.7	5.4
		Envelope		3.4	8.4
		Average	E	5.2	8.4
		Envelope		7.1	14.4
	Combination of far-field and near-field	Average	D	1.8	4.3
		Envelope		2.7	6.8
		Average	E	3.6	5.4
		Envelope		4.5	7.0
ISO	NA	NA	D	1.6	2.4
		NA	E	2.4	4.2

Referring to Table 5, it can be concluded that values of C_a and C_v for soil type E are higher compared to soil type D. Even though seismic events from far-field have a higher magnitude compared to near-field, the distance traveled caused energy loss; thus, the C_a and C_v values from far-field seismic events were found to be the lowest in this study. In contrast with the near-field seismic events, a closer distance led to higher C_a and C_v values even though the magnitude was lower than far-field seismic events. Thus, the combination of far-field and near-field was proposed to avoid overestimating or underestimating C_a and C_v values. Note that the site coefficients were proposed by referring to the methodology in ISO19902-1 [26]. The designed horizontal response spectral acceleration can be presented in the form of a graph or it can be constructed using site coefficients and equations suggested in ISO19902-1.

4. Conclusions

The significant outcome of this study involved the microzonation of the Malay Basin, focusing on soil characteristics to enhance the reliability of the existing offshore facilities in that region. The summary of the findings, with respect to these objectives, are as follows:

- The primary objective was achieved. The soil characteristics based on the study area were analyzed for the Malay Basin, which consisted of soil types D and E. Softer soil possesses the highest value of vibration predicted on the seabed (PSa).
- Objective two was achieved. The soil characteristics based on these data were analyzed. It was confirmed that most of the soil were soil types D and E, which were softer

soil types; these soil types usually give the basin effect, which is an amplification. The soil amplification factors were successfully developed and could be used in the development and maintenance of offshore facilities in the Malay Basin.

- Objective three was achieved. For the design practices and analysis, response spectra are important, and this study developed ‘designed’ horizontal response spectra for the 5% damping ratio because most of the shallow water structures, such as fixed-jacket platforms, fall in this damping ratio.

In conclusion, the aim of this study, which was to develop a seismic microzonation map of the Malay Basin that could be used for the construction and maintenance of offshore facilities, was achieved. It is believed that the proposed peak surface acceleration, soil amplification factor, designed horizontal response spectral acceleration, and site coefficients reflect better the actual site conditions, while the effect of the shaking intensity of soil non-linearity was taken into account. However, further investigations should be commenced, including enhancing the number of well-documented soil profiles, and a simulation of strong motion recordings at different soil site conditions.

It is believed that the proposed peak surface acceleration, soil amplification factor, designed horizontal response spectral acceleration, and site coefficients, reflect the actual site conditions better, while the effect of shaking intensity of soil nonlinearity was taken into account. However, further investigations should be commenced, including enhancing the number of well-documented soil profiles, and a simulation of strong motion recordings at different soil site conditions.

Author Contributions: Conceptualization, M.M.; methodology, M.M.; software, M.M. and K.U.D.; validation, M.M., M.S.L. and A.A.; formal analysis, M.M. and K.U.D.; investigation, A.A. and N.H.A.H.; resources, M.M. and M.S.L.; data curation, M.M. and N.H.A.H.; writing—original draft preparation, M.M. and M.S.L.; writing—review and editing, M.M.; visualization, M.M. and N.H.A.H.; supervision, M.S.L., A.A., N.H.A.H. and K.U.D.; project administration, M.M. and M.S.L.; funding acquisition, M.S.L. All authors have read and agreed to the published version of the manuscript.

Funding: The authors would like to thank the Yayasan Universiti Teknologi PETRONAS-Fundamental research grant (YUTP-FRG)-015LC0-094 and 015LC0-312 for funding this project.

Institutional Review Board Statement: Not applicable.

Informed Consent Statement: Not applicable.

Conflicts of Interest: The authors declare no conflict of interest.

References and Note

1. Che Abas, M.R. Earthquake Monitoring in Malaysia. Presented in Seismic Risk Seminar Malaysia on 25 September 2001.
2. Adnan, A.; Djazilus, H.; Marto, A.; Irsyam, M. Seismic Hazard Assessment for Peninsular. *J. Teknol.* **2005**, *42*, 57–73.
3. Ghani, K.D.A.; Hamid, N.H.A.; Jaafar, M.S. Load versus Displacement Validation between Ruaumoko Hysteresis Program and Experimental Work on CFRP Retrofitted Precast Beam-Column Exterior Joint. *Key Eng. Mater.* **2014**, *594–595*, 390–394. [[CrossRef](#)]
4. Sykes, L.R. Decadal Seismicity Prior to Great Earthquakes at Subduction Zones: Roles of Major Asperities and Low-Coupling Zones. *Int. J. Geosci.* **2021**, *12*, 845–926. [[CrossRef](#)]
5. Sadeghi, K. An Overview of Design, Analysis, Construction and Installation of Offshore Petroleum Platforms Suitable for Cyprus Oil/Gas Fields. *J. Soc. Appl. Sci.* **2007**, *2*, 1–16.
6. Bishop, M.G. *Petroleum Systems of the Malay Basin Province*; US Department of the Interior: Washington, DC, USA, 2002.
7. Madon, M.; Yang, J.-S.; Abolins, P.; Hassan, R.A.; Yakzan, A.M.; Zainal, S.B. Petroleum systems of the Northern Malay Basin. *Bull. Geol. Soc. Malays.* **2006**, *49*, 125–134. [[CrossRef](#)]
8. Ramli, N. The history of offshore hydrocarbon exploration in Malaysia. *Energy* **1985**, *10*, 457–473. [[CrossRef](#)]
9. Sulaiman, N.; Amiruddin, M.A.S.M.; Sulaiman, N.; Khan, M.M.A.; Rosmadi, N.S. Seismic Facies and Geological Structure Interpretation of the A-Field, Malay Basin, Malaysia. *IOP Conf. Ser. Earth Environ. Sci.* **2020**, *549*, 012019. [[CrossRef](#)]
10. Hassaan, M.; Bhattacharya, S.K.; Mathew, M.J.; Siddiqui, N.A. Understanding Basin Evolution through Sediment Accumulation Modeling: A Case Study from Malay Basin. *Res. J. Appl. Sci. Eng. Technol.* **2015**, *11*, 388–395. [[CrossRef](#)]
11. Kong, L.K. Structural analysis of the Malay Basin. *Bull. Geol. Soc. Malays.* **1997**, *40*, 157–176. [[CrossRef](#)]
12. Tjia, H. Growing Evidence of Active Deformation in the Malay Basin Region. *Bull. Geol. Soc. Malays.* **2010**, *56*, 35–40. [[CrossRef](#)]
13. Kurian, V.; Wahab, M.; Voon, M.; Liew, M. Pushover Analysis for Jacket Platform Sensitivity Study and Safety Ratios. Available online: <http://eprints.utp.edu.my/11318/> (accessed on 6 January 2015).

14. Soom, E.M.; Husain, M.K.A.; Zaki, N.I.M.; Nor, M.N.K.M.; Ayob, M.S.; Najafian, G. Global ultimate strength assessment (GUSA) for lifetime extension of ageing offshore structures. *Proc. Int. Offshore Polar Eng. Conf.* **2015**, *2015*, 431–435.
15. Soom, E.M.; Husain, M.K.A.; Zaki, N.I.M.; Nor, M.N.K.M.; Najafian, G. Prediction of Ultimate Shear Strength of Reinforced-Concrete Deep Beams P REDICTION OF U LTIMATE S HEARS S TRENGTH OF R EINFORCED. *Malays. J. Civ. Eng.* **2018**, *30*, 152–171. [[CrossRef](#)]
16. Mihalic, S.; Ostric, M.; Krkac, M. Seismic microzonation: A review of principles and practice. *GEOFIZIKA* **2011**, *28*, 5–20.
17. Govindaraju, L.; Ramana, G.V.; Hanumantharao, C.; Sitharam, T.G. Site-specific Ground Response Analysis. *Spec. Ed. Geotech. Earthq. Hazards* **2004**, *87*, 1354–1362.
18. Beyhan, G.; Keskinsezer, A.; Beyhan, S. A Comparative Study on Soil Properties and Applications Review with EERA and NERA in İstanbul-MARMARAY Project between Kazlıçeşme to Sirkeci. *Period. Eng. Nat. Sci.* **2017**, *5*, 65–80. [[CrossRef](#)]
19. Basu, D.; Dey, A. Comparative 1D Ground Response Analysis of Homogeneous Sandy Stratum Using Linear, Equivalent Linear and Nonlinear Masing Approaches. In Proceedings of the National Seminar on Geotechnics for Infrastructure Development, Kolkata, West Bengal, India, 11–12 March 2016.
20. Marto, A.; Adnan, A.; Hendriyawan, H.; Irsyam, M. Microzonation Maps for Kuala Lumpur and Putrajaya. *Malays. J. Civ. Eng.* **2011**, *23*, 63–85.
21. Adnan, A.; Hendriyawan; Marto, A. *Development of Microzonation Maps of Kuala Lumpur City Centre for Seismic Design of Buildings*; The Institution of Engineers: Selangor, Malaysia, 2008; pp. 12–15.
22. Irsyam, M.; Dangkoa, D.T.; Hoedajanto, D. Proposed seismic hazard maps of Sumatra and Java islands and microzonation study of Jakarta city, Indonesia. *J. Earth Syst. Sci.* **2008**, *117*, 865–878. [[CrossRef](#)]
23. First, S.; Isik, N.S.; Arman, H.; Demir, M.; Vural, I. Investigation of the Soil Amplification Factor in the Adapazari Region. *Bull. Eng. Geol. Environ.* **2015**, *75*, 141–152. [[CrossRef](#)]
24. Kramer, S.L. *Geotechnical Earthquake Engineering*; Prentice Hall: Hoboken, NJ, USA, 1996.
25. Adrian, R.-M.; Jonathan, D.B.; Norman, A.A. A Geotechnical Seismic Site Response Evaluation Procedure. In Proceedings of the Twelfth World Conference on Earthquake Engineering, Auckland, New Zealand, 30 January–4 February 2000; Volume 14, p. 1590. Available online: <http://www.iitk.ac.in/nicee/wcee/article/1590.pdf> (accessed on 8 November 2017).
26. *ISO 19901-2; Petroleum and Natural Gas Industries—Specific Requirements for Offshore Structures—Part 2: Seismic Design Procedures and Criteria*. American National Standards Institute: New York, NY, USA, 2004.
27. Freeman, S.A. Response Spectra as a Useful Design and Analysis Tool for Practicing Structural Engineers. *ASET J. Earthq. Technol.* **2007**, *44*, 25–37.
28. Chang, B.; Abraham, M.; Peng, B.; Engineering, J.R.M. Comparison of ISO and API Seismic Design Guidelines Using Three Existing Offshore Platforms. In Proceedings of the Offshore Technology Conference, Houston, TX, USA, 2–5 May 2005. [[CrossRef](#)]
29. Villaverde, R. *Fundamental Concepts of Earthquake Engineering*, 1st ed.; CRC Press—Taylor & Francis Group: Boca Raton, FL, USA, 2009.
30. Hegazy, Y.A.; Mayne, P.W. Statistical Correlations Between Vs and CPT Data for Different Soil Types. In Proceedings of the International Symposium on Cone Penetration Testing: CPT'95, Linköping, Sweden, 4–5 October 1995; Volume 2, pp. 173–178.
31. Mayne, P.W. In-situ test calibrations for evaluating soil parameters. In Proceedings of the Characterization and Engineering Properties of Natural Soils II, Singapore, 29 November–1 December 2006; pp. 1601–1652.
32. Sykora, D.W. Examination of Existing Shear Wave Velocity and Shear Modulus Correlations in Soils, Vicksburg, Mississippi, 1987. Available online: www.dtic.mil/get-tr-doc/pdf?AD=ADA214721 (accessed on 17 November 2017).
33. Hoe, L.Y. *Soil Amplification Factor of Seismic Ground Motions in Laho (PMO), Kumang (SKO) and Sumandak (SBO) in Malaysian Offshore*; IRC, Universiti Teknologi PETRONAS: Perak, Malaysia, 2015.
34. Organisation of Educational Cooperation. *Seismic Hazard study and Zoning of Offshore Location in Malaysia: Peninsular Malaysia, Sarawak and Sabah Operations*; Organisation of Educational Cooperation: Perak, Malaysia, 2014.
35. Bardet, J.P.; Tobita, T. NERA A Computer Program for Nonlinear Earthquake site Response Analyses of Layered Soil Deposits. Department of Civil Engineering, University of Southern California. 2001. Available online: <https://sites.google.com/site/tt60898/home/software> (accessed on 28 April 2016).
36. Lam, N.; Tsang, H.H.; Looi, D.; Lumantara, E.; Wilson, J. Seismic Hazard Modelling for Malaysia and Singapore. In Proceedings of the 2017 World Congress on Advances in Structural Engineering and Mechanics (ASEM17), Ilsan, Korea, 28 August–1 September 2017.
37. Nabilah, A.B.; Koh, C.G.; Safiee, N.A.; Daud, N.N.N. *Site Specific Seismic Hazard Assessment for Kuala Lumpur And Vicinity from Long Distance Earthquakes*, no. *Special Publication for NCWE2017*; Faculty of Civil Engineering & Earth Resources, University Malaysia Pahang (UMP): Pekan, Malaysia, 2017; pp. 15–20.
38. Loi, D.W.; Raghunandan, M.E.; Swamy, V. Revisiting seismic hazard assessment for Peninsular Malaysia using deterministic and probabilistic approaches. *Nat. Hazards Earth Syst. Sci.* **2018**, *18*, 2387–2408. [[CrossRef](#)]
39. Carlton, B.; Barwise, A.; Kaynia, A.M. Seismic Hazard Assessment for a Wind Farm Offshore England. *Geotechnics* **2022**, *2*, 14–31. [[CrossRef](#)]
40. Birkmann, J. *Measuring Vulnerability to Natural Hazards*; United Nations University Press: Tokyo, Japan, 2013.
41. Thitimakorn, T.; Raenak, T. NEHRP Site Classification and Preliminary Soil Amplification Maps of Lamphun City, Northern Thailand. *Open Geosci.* **2016**, *8*, 538–547. [[CrossRef](#)]

42. Yunita, H.; Setiawan, B.; Saidi, T.; Abdullah, N. Site response analysis for estimating seismic site amplification in the case of Banda Aceh—Indonesia. In Proceedings of the AASEC 2018 The 3rd Annual Applied Science and Engineering Conference, Bandung, Indonesia, 18 April 2018; Volume 10002, pp. 1–6.
43. Majid, T.A.; Zaini, S.S.; Nazri, F.M.; Arshad, M.R.; Suhaimi, I.F.M. Development of Design Response Spectra for Northern Peninsular Malaysia Based on UBC 97 Code. *Inst. Eng. Malays.* **2007**, *68*, 23–29.
44. Asakereh, A.; Jamali, H.; Naderi, E. The Influence of Seismic Parameters on Site Response. *Civ. Eng. Dimens.* **2015**, *17*, 76–87. [[CrossRef](#)]
45. Yunita, H.; Djazilus, H.; Apriadi, D. An Overview of Soil Models for Earthquake Response Analysis. *J. Eng. Technol. Sci.* **2015**, *47*, 57–75. Available online: <http://journals.itb.ac.id/index.php/jets/article/view/362/782> (accessed on 25 July 2021). [[CrossRef](#)]